Environmental Pollution 255 (2019) 113192

Contents lists available at ScienceDirect

Environmental Pollution

journal homepage: www.elsevier.com/locate/envpol

Adsorption and fractionation of Pt, Pd and Rh onto inorganic microparticles and the effects of macromolecular organic compounds in seawater☆

Kai Liu [a, b, c], Xuelu Gao [a, b, *]

[a] CAS Key Laboratory of Coastal Environmental Processes and Ecological Remediation, Yantai Institute of Coastal Zone Research, Chinese Academy of Sciences, Yantai, Shandong, 264003, China
[b] University of Chinese Academy of Sciences, Chinese Academy of Sciences, Beijing, 100049, China
[c] Dongying Municipal Bureau of Marine Development and Fisheries, Dongying, Shandong 257000, China

ARTICLE INFO

Article history:
Received 30 October 2018
Received in revised form
5 September 2019
Accepted 5 September 2019
Available online 10 September 2019

Keywords:
Adsorption
Fractionation
Inorganic microparticles
Macromolecular organic compounds
Platinum group elements
Seawater

ABSTRACT

Adsorption and fractionation of Pt, Pd and Rh (defined here as platinum group elements, PGEs) onto the representative inorganic microparticles, including Fe_2O_3, MnO_2, $CaCO_3$, SiO_2, Al_2O_3 and kaolinite in seawater were investigated. The effects of macromolecular organic compounds (MOCs) as the representatives of organic matter, including humic acids (HA), bovine serum albumin (BSA) and carrageenan, on the adsorption were also studied considering that organic matter is ubiquitous in seawater and indispensable to marine biogeochemical cycles. In the absence of MOCs, the representative mineral particles Fe_2O_3 and MnO_2 had the strongest interaction with PGEs. The adsorption of PGEs onto the representative biogenic particles SiO_2 and $CaCO_3$ and lithogenic particles Al_2O_3 and kaolinite was similar or weaker than onto the mineral particles. MOCs inhibited the interaction between PGEs and the particles except for Pt and Pd onto the biogenic particles in artificial seawater. This impediment may be closely related to the interaction between particles, MOCs and elements. The partition coefficient ($\log K_d$) of Pt was similar (~4.0) in the presence of MOCs, indicating that the complexation between Pt and MOCs was less important than hydrolysis or adsorption onto the acid oxide particle surface. Rh tended to fractionate onto the mineral and lithogenic particles in the presence of HA and carrageenan, while Pd was more likely to fractionate onto the biogenic particles. However, BSA enhanced the fractionation tendency of Pd onto the mineral particles. The results indicate that the adsorption behavior of Pd onto inorganic particles was significantly affected by the composition or the type of MOCs. Hence, the interaction between PGEs and inorganic particles may be greatly affected by the macromolecular organic matter in the ocean.

1. Introduction

There has been a huge increase in three anthropogenically derived platinum group elements (PGEs) in natural environments, namely Pt, Pd and Rh, because of their wide application in anticancer drugs, chemical catalysis, and especially automotive catalytic converters (Koek et al., 2010; Mudd, 2012; Pawlak et al., 2014; Speder et al., 2014). Owing to the potential hazards of these pollutants to humans (Merget and Rosner, 2001; Wiseman and Zereini, 2009; Sorensen et al., 2016; Zimmermann et al., 2017), researchers have investigated the biogeochemical behaviors of PGEs in various environmental matrixes (Reith et al., 2014). Furthermore, a migration path of these elements in the environment, vehicle exhaust—soil—aquatic system, was preliminarily defined (Mitra and Sen, 2017). Tiny particulate PGEs have been released from vehicles into the atmosphere in the abrasion and deterioration of catalysts and subsequently enter the soil with atmospheric deposition and rainfall (Colombo et al., 2008; Wiseman and Zereini, 2009; Pawlak et al., 2014; Clement et al., 2015; Ruchter and Sures, 2015). Later, PGEs in their elemental states are transformed

☆ This paper has been recommended for acceptance by Dr. Jörg Rinklebe.

* Corresponding author. CAS Key Laboratory of Coastal Environmental Processes and Ecological Remediation, Yantai Institute of Coastal Zone Research, Chinese Academy of Sciences, Yantai, Shandong, 264003, China.
E-mail address: xlgao@yic.ac.cn (X. Gao).

https://doi.org/10.1016/j.envpol.2019.113192
0269-7491/

into oxidation states with the compounds present in soil (Ek et al., 2004; Šebek et al., 2011; Sucha et al., 2016). Finally, PGEs enter the aquatic environments such as rivers, estuaries and seawater with runoff and rainfall (Pawlak et al., 2014; Ruchter and Sures, 2015; Mitra and Sen., 2017). Moreover, PGEs have the characteristics of forming complexes easily with donor ligands such as suspended particulate matter (SPM) and dissolved organic matter (DOM) present in the natural aquatic system (Baker and Spencer, 2004; Turner et al., 2006; Turner and Wu, 2007). Hence, biogeochemical behaviors of PGEs in aquatic systems could dramatically affect the status of these elements in the environment. However, there is a lack of the information about the interactions between PGEs and SPM or DOM, because the detection of PGEs is restricted at typical environmental levels (Rao and Reddi, 2000; Suzuki et al., 2014; Fornieles et al., 2016; Mashio et al., 2016).

Some researchers have explored the role of SPM or sediment in the scavenging of PGEs in aquatic systems. Turner et al. (2006) reported that the adsorption of PGEs onto suspended estuarine sediment was dominated by the hydrous metal oxides of the particles in filtered river water. However, it was also found that the adsorption process was significantly controlled by the complexation of PGEs with natural organic ligands (Turner et al., 2006). The organic ligands might alter the surface characteristics of the particles and the complexation of PGEs present in the river water (Turner and Wu, 2007). These interactions would notably influence the mobilization of PGEs between SPM and water (Cobelo-García et al., 2013; Cobelo-García et al., 2014). Nevertheless, the compositions of SPM and DOM in natural aquatic environments were found varying with seasons, locations and input conditions. And DOM would change the surface characteristics of SPM, influencing the migration of PGEs in SPM-water system. However, most research focused on the interaction between elements and sinking particles collected with sediment traps, and the role of organic matter, which is critical for the understanding of the pollution and risk of PGEs in environments, has not been explored (Turner et al., 2006; Turner and Wu, 2007; Cobelo-García et al., 2013; Cobelo-García et al., 2014).

In this research, controlled adsorption experiments were conducted for the investigation of the adsorption of PGEs in seawater with the presence of different types of inorganic microparticles and DOM. The microparticles used in this study represented the composition of inorganic SPM in seawater essentially (Lardinois et al., 1995). SiO_2 and $CaCO_3$ represented the biogenic component, Al_2O_3 and kaolinite were the lithogenic component, and the mineral fraction was represented by Fe_2O_3 and MnO_2 (Yang et al., 2013; Lin et al., 2014; Lin et al., 2015; Yang et al., 2015). Comparative experiments were conducted in the presence of diverse DOM for the investigation of the role of organic matter in regulating this adsorption in seawater. The organic matter used in this study was some model MOCs, namely humic acid (HA), bovine serum albumin (BSA) and carrageenan (Sigma-Aldrich® Product Number C1867), which represented the known major substances of natural DOM including humic matter, protein and acid polysaccharides, respectively (Gueguen et al., 2006; Yang et al., 2013; Ilina et al., 2014; Lin et al., 2014; Lin et al., 2015; Yang et al., 2015). This study focused on the role of the chemical components of particles and DOM in the fractionation of PGEs in seawater; the effects of living organisms and the precipitation of PGEs were not taken into account; in addition, the electrical potential of the solutions was simply regarded as qualitative evidence and not taken into deep discussion.

2. Materials and methods

2.1. Reagents and seawater

The microparticles and MOCs selected for the adsorption experiment are representatives of the major known particulate and DOM components in seawater (Yang et al., 2013; Lin et al., 2015). The characteristics of MOCs including the main constituents, functional groups and molecular weights are shown in Table 1; the details of microparticles including the surface area and zeta potential are shown in Table 2. The ultrapure deionized water (DIW, >18 MΩ-cm) used in this study was prepared with a Pall® Cascada™ water purification system.

The mixed stock solution of 1 mg L^{-1} each of Pt, Pd and Rh was prepared in 2 mol L^{-1} HCl in a 1 L high-density polyethylene bottle (Thermo®) with a standard of 1000 mg L^{-1} individual elements of Pt, Pd and Rh supplied by General Research Institute for Nonferrous Metals, China. The chemical forms of Pt, Pd and Rh in the stock solution were Cl-forms and the oxidation states were +2, +2 and + 3, respectively. The labwares used in this study were cleaned strictly according to Li et al. (2015) and Liu et al. (2019). They were washed with Decon® 90 (2% in DIW), then infused in 10% HNO_3 and 10% HCl for 48 h, followed by rinsing with DIW for more than five times, and finally dried in a Class 100 clean bench.

For comparison, two solution systems were applied, one prepared with artificial seawater (ASW) which did not contain organic

Table 1
Characteristics of macromolecular organic components used in this research.

Macromolecular organic matter	Represented component of DOM	Main functional group	Molecular weight	Provider
Humic acid sodium salt	Humic matter	$-COO^-$	>10 kDa	Sigma-Aldrich China, Inc.
Bovine serum albumin	Protein	Amino acid residue	~66.4 kDa	Shanghai Luoshen Biological Technology Co. Ltd
Mixture of κ- and λ-carrageenans	Acid polysaccharides	$=-OSO_3^-$, $-OH$	>20 kDa	Sigma-Aldrich China, Inc.

Table 2
Characteristics of inorganic microparticles used in this research.

Particle	Median grain size (μm)	Specific surface area (m^2 g^{-1})	Zeta potential in ASW (mV)	Zeta potential in UVSW (mV)	Provider
Fe_2O_3	7.1	23.8	−6.82	2.16	Sinopharm Chemical Reagent Co., Ltd
MnO_2	11.6	18.9	−5.47	−3.53	Sinopharm Chemical Reagent Co., Ltd
$CaCO_3$	11.1	2.56	14.50	10.80	Sinopharm Chemical Reagent Co., Ltd
SiO_2	2.6	2.12	−15.60	−8.10	Sinopharm Chemical Reagent Co., Ltd
Al_2O_3	8.0	21.3	−6.78	−4.64	Sinopharm Chemical Reagent Co., Ltd
Kaolinite	9.5	35.7	−5.78	−3.45	Sinopharm Chemical Reagent Co., Ltd

matter and nutrients and the other prepared with ultraviolet irradiated natural seawater (UVSW) from which DOM was removed. ASW was prepared according to the method D1141-98, Reapproved 2013 (American Society for Testing and Materials, ASTM). UVSW was prepared by irradiating natural seawater under ultraviolet light (500 W) for over 48 h to remove most of the active DOM, and the residual background concentration of dissolved organic carbon in UVSW was less than 0.2 mg L^{-1}. The natural seawater was collected from the North Yellow Sea (123.912°E, 38.965°N), filtered through a 0.2 μm hydrophilic polyethersulfone membrane (Pall®) and stored in 4 L polypropylene (PP) bottle (Thermo®) at 4 °C for further use.

2.2. Adsorption studies

The adsorption experiment was operated in 100 ml Teflon beakers with lid. Teflon was reported to have low surface adsorption of PGEs ions (Cobelo-García et al., 2008). The adsorption procedures are schematized in Fig. 1. The experimental preparations were performed in the clean bench. The adsorption was conducted at room temperature (20 ± 2 °C) in the dark under two conditions: single kind of particle system and particle-MOC system. The following is the brief account of the experimental procedure. 48.5 ml of ASW or UVSW were added into 100 ml Teflon beakers, and then each was spiked in 1 ml non-complexing Tris-HCl buffer (pH ~8.5). The buffer could maintain the pH of the experimental solution at ~8.2 and prevent the irreversible formation of interfering colloids, caused by pH drift, which could significantly influence the adsorption of PGEs onto particles (Roberts et al., 2009; Yang et al., 2013; Li et al., 2015).

For a single kind of microparticle system, 2.5 ± 0.05 mg of particles was added into each of the 100 ml Teflon beakers. The final concentration of particles was 50 mg L^{-1}, which was close to the general SPM concentration (1–100 mg L^{-1}) in natural seawater (Yang et al., 2013). Then, 0.5 ml of PGEs stock solution was added to make the work concentration of each Pt, Pd and Rh at 10 μg L^{-1}. The final experimental solution volume was 50 ml. Notably, 10 μg L^{-1} of PGEs was dramatically higher than the natural concentration of these elements in the ocean. Nevertheless, this concentration was comparable to that of some other trace elements in seawater and lower enough compared with the concentration of ligands that could potentially bind with PGEs (Turner et al., 2006; Turner and Wu, 2007). Hence, the experimental condition could, at least to some extent, reflect the adsorption situation of PGEs in seawater (Turner et al., 2006; Turner and Wu, 2007). Furthermore, this concentration is necessary to allow for an interference-free detection by inductively coupled plasma mass spectrometry (ICP-MS) (Turner et al., 2006). Base on the results of pre-experiments (Fig. S1), the solutions were shaken for about 12 h in the dark for adsorption equilibrium. After the adsorption, the particles and the work solution were separated through filtration with a 0.45 μm pre-weighted hydrophilic polyethersulfone membrane (PALL®). The filtration device was pretreated with 10 ml of work solution three times to reduce the retention of PGEs (Turner et al., 2006; Turner and Wu, 2007). 5 ml of filtrates were pipetted into 15 ml pre-weighed polypropylene (PP, FCOLON™) centrifuge tubes, diluted to 10 ml by 2% HCl, and stored at 4 °C. The particles retained on the membranes were dried in the clean bench for 24 h and weighted to calculate the mass balance of the particles. The weighted membranes were soaked in 10 ml of 2.5 M HCl in 15 ml PP centrifuge tubes at room temperature to be digested for one week. After the digestion, the tubes were centrifuged at 2500 rpm for 5 min. And then, 5 ml of supernatants were pipetted to 15 ml PP centrifuge tubes and stored at 4 °C.

The role of MOCs in the fractionation of PGEs onto inorganic microparticles was investigated with the binary experiments in which the microparticle and MOCs were simultaneously added into the adsorption solutions and stirred for 30 min before spiking PGEs, guaranteeing the sufficient interaction between MOCs and microparticles (Yang et al., 2013). The final concentration of MOCs was 2 mg L^{-1}, which was in the range of natural DOC concentrations of 1.09–4.22 mg L^{-1} in the Bohai and Yellow Seas (Ran et al., 2013; Liu et al., 2015). Other procedures were the same as the single kind of particle system. The control experiments were conducted simultaneously in which the same concentrations of PGEs as that of the single kind of particle and particle-MOC experiments were spiked but no microparticles and MOCs were added.

The pH throughout the adsorption experiments was monitored with a Meteler Toledo® pH meter, because Cobelo-García et al. (2008) reported that significant changes in pH may lead to undesirable colloid formation, particle dissolution, and precipitation of PGEs in the solution, which interfere in the adsorption dramatically, and the sample must be discarded if the pH of the experimental system drifted more than ~0.3 pH units. Three repeated operations were conducted simultaneously for each adsorption process.

2.3. Sample analysis

The concentration of Pt, Pd and Rh in filtrates and digestions was

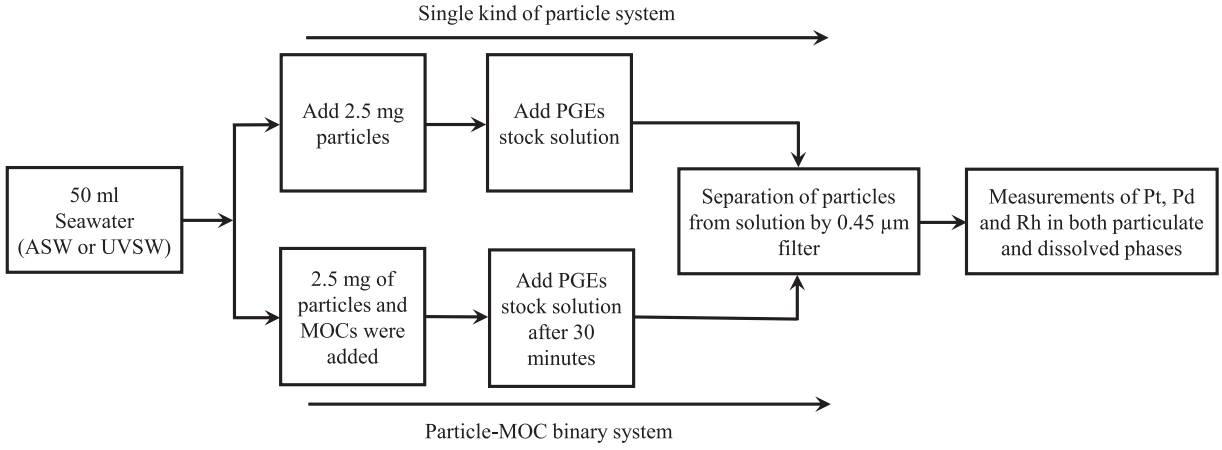

Fig. 1. Schematic diagram of the adsorption experiments for investigating the partitioning of Pt, Pd and Rh between seawater and inorganic microparticles.

analyzed with ICP-MS (ELAN DRC II, PerkinElmer®). The filtrates were diluted 25-fold in 2% HNO_3 to maintain the concentration of dissolved salt being <0.1% w/v to minimize signal interference from the saline matrix. The digestions were diluted to twice their original volumes with DIW. The instrument was calibrated using 2% HNO_3-based multi-element standards which were prepared with UVSW and ASW, and ^{115}In was added as the internal standard to make a concentration of 10 μg L^{-1}. The concentrations of Pt, Pd and Rh were determined with the signal of ^{103}Rh, the average signals of ^{194}Pt and ^{195}Pt, and ^{106}Pd and ^{108}Pd, respectively (Djingova et al., 2003). A standard and a blank were inserted in every analysis of the 12 samples to monitor the instrument errors.

The zeta potential of the solutions was determined with a Malvern Panalytical® Nano-ZS90 analyzer. The surface morphology of the particles was obtained with a Hitachi® S-4800 high-resolution scanning electron microscope (SEM). The work conditions of the microscope were 3 kV accelerating voltage, 2,000–100,000 × magnification, 3800–4200 μm working distance and 6,000–10,000 nA emission current. In this study, the images with a magnification of 50,000 × were selected for the analysis, which clearly reflected the surface conditions of the particles.

2.4. Recovery, partition coefficient, and fractionation factor

The mass recovery was used to measure the adsorption of PGEs onto the container walls and the experimental operation on the adsorption results (Yang et al., 2013). The total recovery was defined as R to evaluate the loss of PGEs during the experiment:

$$R = \frac{M_s + M_P}{M_I} \times 100\%$$

where R represents the ratio of the total mass recovery of PGEs before and after the adsorption; M_s represents the mass of PGEs in the liquid phase after adsorption; M_p represents the mass of PGEs in the particulate phase after adsorption; M_I represents the initial mass of PGEs added to the solution. When R = 100%, there is no loss of PGEs in the experiment; when R < 100%, there is some loss; the greater the difference between R and 100% is, the greater loss occurs in the experiment.

The partition coefficient (K_d) of PGEs between seawater and particulate phases was calculated with a traditional formulation which has been used in different experimental systems (Honeyman and Santschi, 1989; Yang et al., 2013):

$$K_d = \frac{C_p}{C_d C_T}$$

where C_P represents the concentrations of PGEs in the particulate phase; C_d is the concentrations of PGEs in the dissolved phase; C_T is the total concentrations of microparticles in the solution. The K_d values (in L kg^{-1}) are reported in terms of log K_d.

The fractionation factor (F) was defined as the ratio of K_d values to evaluate the fractionation behavior of those elements by a specific microparticle (Yang et al., 2013; Lin et al., 2015):

$$F_{A/B} = \frac{K_{d,A}}{K_{d,B}}$$

where $K_{d,A}$ and $K_{d,B}$ are the partition coefficients of PGE A and B, respectively; $F_{A/B}$ is the fractionation factor between A and B. When $F_{A/B} = 1$, there is no fractionation in that particular particle during adsorption. When the $F_{A/B} > 1$ or <1, the particle preferentially absorbs PGE A over B or B over A.

3. Results

3.1. The recovery of Pt, Pd and Rh

The R value of each PGE was measured for the evaluation of its loss in the experiments, and the results under different experiment conditions are shown in Fig. 2. Overall, R ranged from 80 to 100% and varied with different elements, which means that experimental design and operation satisfied the objectives of this research.

The R values of Pt in all conditions were higher than 90%, indicating that no significant loss of Pt occurred during the adsorption experiment. For Pd, a different feature of R was found with the addition of MOCs in ASW (Fig. 2). In the absence of MOCs, most of the R values of Pd were ~95%. But a slight increase about 2–3% was observed with the addition of MOCs. It may be due to the impeding effects of MOCs on the adsorption of Pd onto the container walls (Cobelo-García et al., 2008). The organic complexation formed between MOCs and Pd had a stronger solvability than the inorganic complexes of Pd (Wood, 1996; Colombo et al., 2008).

For Rh, a wider range of R value about 80–95% was observed and varied with the experimental conditions (Fig. 2). It indicated that relatively lower R values were generally obtained in the presence of MOCs, which might be caused by the Rh adsorption onto container walls, the precipitation of Rh complexes (Cobelo-García et al., 2008; Colombo et al., 2008) and other unknown factors during the experimental operation.

3.2. Partition coefficient of Pt, Pd and Rh

The partition coefficient of Pt, Pd and Rh could reflect an intuitive adsorption behavior of PGEs onto the particles. In this study, the log K_d varied with the types of organic matter, element and particles, and the results are shown in Table S1 and Fig. 3.

The strongest adsorption occurred in the interaction between PGEs and MnO_2 in UVSW, with the log K_d value being greater than 5.7, followed by Fe_2O_3 being approximately 5.6. The lowest adsorption occurred on the Al_2O_3 particles and the log K_d was about 3.89 ± 0.02 (Fig. 3 and Table S1). The interactions between the studied PGEs and SiO_2, $CaCO_3$ and kaolinite particles were weaker than mineral particles and the log K_d values ranged from 4.11 to 4.57. Moreover, the fractionation of PGEs onto different particles in ASW and UVSW were diverse.

For Pt, the log K_d on each particle in ASW and UVSW was similar. However, a slight decrease in the coefficient value by ~0.04–0.15 was observed in ASW compared to in UVSW except for SiO_2 with ~0.07 increase in log K_d. For Pd, a larger change of log K_d by 0.06–0.33 appeared. In UVSW, the adsorption of Pd onto Fe/Mn oxides was weaker than in ASW (log K_d decreased by ~0.32), but its adsorption onto biogenic particles were stronger (log K_d increased by ~0.22); besides, the adsorption of Pd onto lithogenic particles were comparable in ASW and UVSW (log K_d changed by ~0.05). For Rh, an obvious difference in its adsorption onto Fe/Mn oxides in ASW and UVSW was observed and the variation of log K_d was about 0.38–0.40; however, its adsorption onto lithogenic and biogenic particles differed slightly in the two seawater conditions expect for Al_2O_3, with the log K_d increased ~0.16 in UVSW. From the above results, it could be obtained that the variation in adsorption reactivity of PGEs onto particles might be related to the residual dissolved organic matter in UVSW, which was the main difference between UVSW and ASW.

In the particle-MOC binary systems, in general, MOCs weakened the adsorption of PGEs onto particles (Fig. 3), and the interactions among them varied greatly. All comparisons in the following were made with the corresponding particle system.

For Rh, the strong adsorption still occurred on the Fe/Mn oxides.

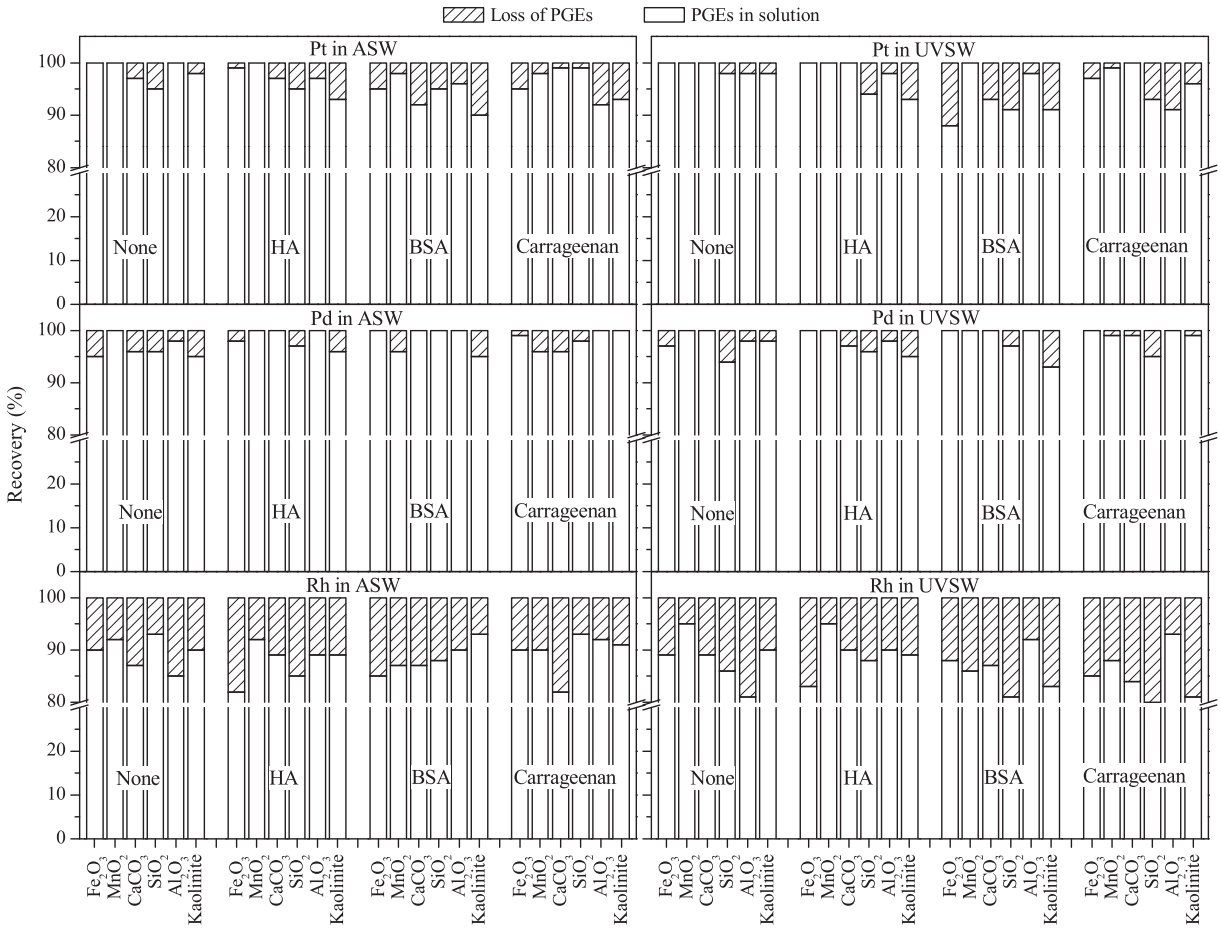

Fig. 2. Recovery of Pt, Pd and Rh in different experimental conditions. Loss of PGEs: the proportion of PGEs that was not determined in both dissolved and particulate phases; PGEs in solution: the sum of PGEs determined in both dissolved and particulate phases. ASW: artificial seawater; UVSW: UV-irradiated natural seawater; None: the particle systems without macromolecular organic compound; HA: the particle systems with humic acid; BSA: the particle systems with bovine serum albumin; Carrageenan: the particle systems with carrageenan.

The log K_d of these binary systems decreased by about 0.47−1.00 and tended to have very similar values of 4.79 ± 0.06 except for the ones with carrageenan in ASW. For the adsorption of Rh onto biogenic particles, MOCs hindered its interaction with $CaCO_3$ in ASW, and log K_d decreased correspondingly by 0.38−0.4; however, they strengthened the adsorption in UVSW and the maximum change of log K_d, about 0.10−0.25, occurred in the systems containing HA. Moreover, the promoting effects of carrageenan and BSA on the distribution of Rh onto $CaCO_3$ particles were similar (Fig. 3). For the interaction between PGEs and SiO_2, HA promoted the adsorption, BSA hindered the adsorption and carrageenan had no effects on the adsorption in ASW, respectively (Fig. 3); in UVSW, MOCs showed only hindering effects on the adsorption, and log K_d decreased by about 0.13−0.28. For the adsorption of Rh onto Al_2O_3, MOCs did not change the interaction obviously, except for HA in ASW which showed the promoting effects and the log K_d increased by 0.1 (Fig. 3 and Table S1). However, MOCs hindered the adsorption of PGEs onto kaolinite, and this inhibition in UVSW was weaker than that in ASW.

For Pd, MOCs inhibited its adsorption onto particles and the decrease of log K_d was 0.10−1.40. Among them, the strongest inhibition effect was on mineral particles (Fig. 3), with the decrease of log K_d by 0.40−1.40, followed by lithogenic particles, with the decrease of log K_d by 0.09−0.63. The weakest hindering effects of MOCs were on the distribution of Pd onto biogenic particles, with the decrease of log K_d being only 0.03−0.34; but there was an exception to this, MOCs slightly promoted the interaction between Pd and $CaCO_3$ in ASW, and the log K_d increased by about 0.1. Additionally, when MOCs were added, the strongest adsorption changed from between Pd and mineral particles (log K_d was 3.21−4.29) to between Pd and biogenic particles (log K_d was 4.12−4.56).

For Pt, the weakening effects of MOCs on the interactions between particles and PGEs were also observed, and the biggest decrease in log K_d by 0.47−1.03 was also on the mineral particles (Fig. 3 and Table S1). The log K_d of lithogenic and biogenic particles was 3.91−4.38 in the presence of MOCs and the fluctuation was no more than 0.2−0.4 (Table S1). The log K_d of the adsorption of Pt onto Fe/Mn oxides in ASW was higher than that in UVSW, and slight promoting effects on the adsorption of Pt onto SiO_2 in ASW were observed (Fig. 3).

In general, MOCs changed to a certain extent the adsorption of PGEs onto inorganic particles, and this effect was closely related to the type of particles and organic matter. This suggested that MOCs had a profound influence on the partition of Rh, Pd and Pt between the particles and the seawater.

3.3. Fractionation factors between Pt, Pd and Rh

Fractionation factors (F) between Pt, Pd and Rh which were derived from their K_d values and expressed by the pairs of Rh−Pd ($F_{Rh/Pd}$), Rh−Pt ($F_{Rh/Pt}$) and Pd−Pt ($F_{Pd/Pt}$) are shown in Fig. 4 and

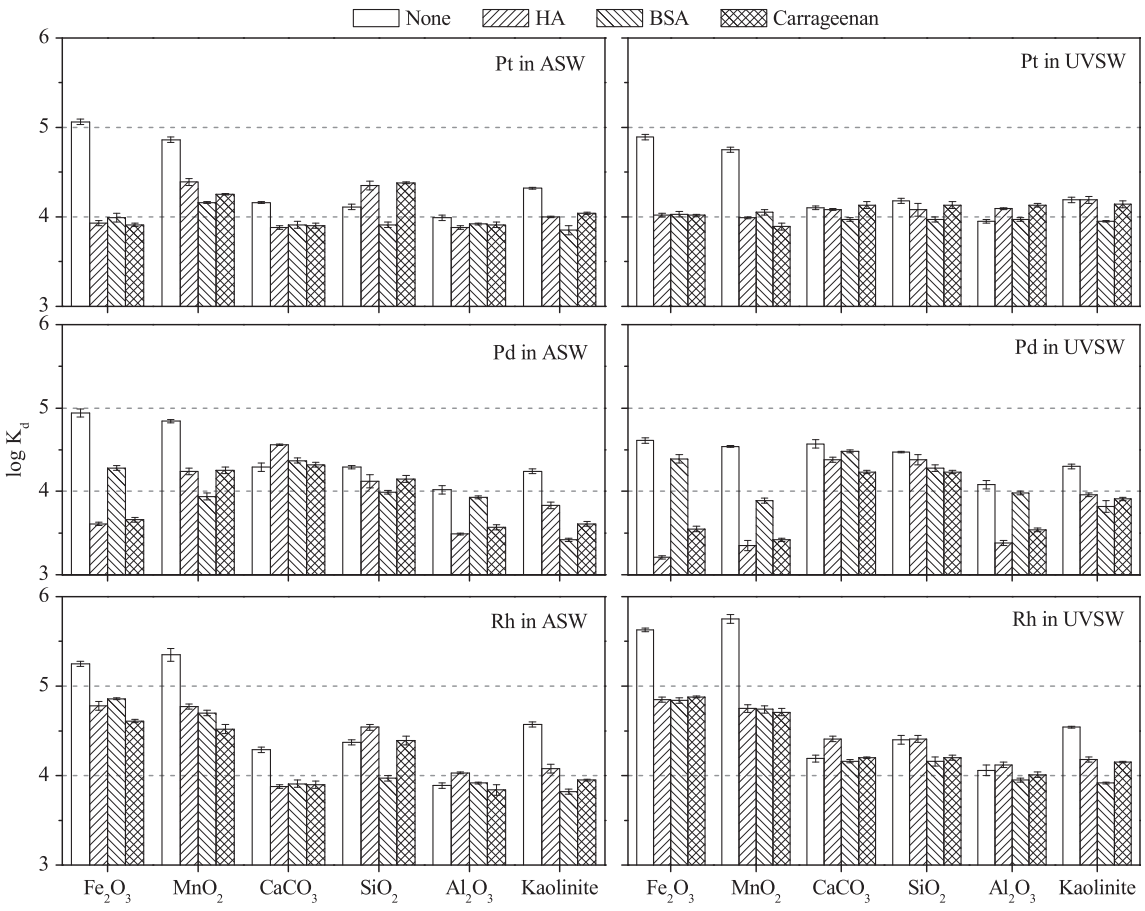

Fig. 3. log K_d of the adsorption of Pt, Pd and Rh onto inorganic microparticles in the presence of macromolecular organic compounds in different seawater solutions. ASW: artificial seawater; UVSW: UV-irradiated natural seawater; None: the particle systems without macromolecular organic compound; HA: the particle systems with humic acid; BSA: the particle systems with bovine serum albumin; Carrageenan: the particle systems with carrageenan.

Table S2. This parameter reflects the adsorption inclination of particles to elements in different environments. The more the F value deviated from 1, the more obvious fractionation of the PGEs onto the tested particles was.

In a single kind of particle system, F of PGEs adsorption onto MnO_2 had the largest value and was obviously higher in UVSW than in ASW except for Pt-Pd. It indicated that the fractionation between Pt and Pd was not significantly affected by the solution matrix. In addition, the difference in F values of PGEs adsorption onto other particles were not significant. In general, the fractionation of PGEs onto Fe_2O_3 and MnO_2 in ASW and UVSW showed a big difference (Table S2).

In the particle-MOC binary systems, MOCs dramatically changed the fractionation between PGEs, and a significant difference between the two seawater conditions was also observed. For Fe_2O_3, F increased in the presence of HA, carrageenan and BSA in ASW; but in UVSW, the effects of MOCs varied: HA and carrageenan enhanced (F increased by 10–30) while BSA inhibited (F decreased by 8) the fractionation between Rh and Pd. The enhancing effect in ASW was significantly stronger than in UVSW. For MnO_2, the effect of MOCs on the fractionation between PGEs in UVSW was similar to that of Fe_2O_3; in ASW, HA and BSA slightly enhanced the fractionation between PGEs (F increased by 0.15–2.5) but carrageenan weakened it (F decreased by about 1).

For biogenic particles, the effect of MOCs in ASW and UVSW also varied significantly. MOCs enhanced the fractionation between PGEs in the process of their adsorption onto $CaCO_3$ in ASW; however, this effect only occurred in the presence of BSA in UVSW. The influence of MOCs on the fractionation between PGEs in the process of their adsorption onto SiO_2 was more complicated: in ASW, HA and carrageenan made a slight enhancement on the fractionation but BSA had no effects; in UVSW, conversely, BSA had an obvious enhancement but carrageenan and HA had almost no effects.

For lithogenic particles, MOCs had a similar effect on the fractionation between PGEs in ASW and UVSW with HA and carrageenan promoting the fractionation but BSA having no obvious effects. The fractionation between the pairs of Rh-Pd and Pd-Pt was promoted more in UVSW than in ASW.

The results revealed that, on the whole, MOCs impacted especially on the fractionation of PGEs in adsorbing onto Fe_2O_3 and MnO_2. The highest F about 43.65 was observed in Fe_2O_3-HA system and followed by that in MnO_2-HA system about 25.11 (Fig. 4). It indicated a very important role of HA in regulating PGEs adsorption onto mineral particles in seawater. For other MOCs, the enhancement of BSA for the adsorption of PGEs onto the particles was higher than that of carrageenan. Hence, the ability of MOCs to affect the adsorption of PGEs onto mineral particles was HA > BSA > carrageenan. But for lithogenic particles, the order changed to be HA > BSA ≈ carrageenan. For biogenic particles, there were different behaviors in the presence of MOCs. The adsorption of PGEs onto $CaCO_3$ was more influenced by MOCs compared with their adsorption onto SiO_2. The ability of MOCs to affect the adsorption of PGEs onto $CaCO_3$ and SiO_2 was

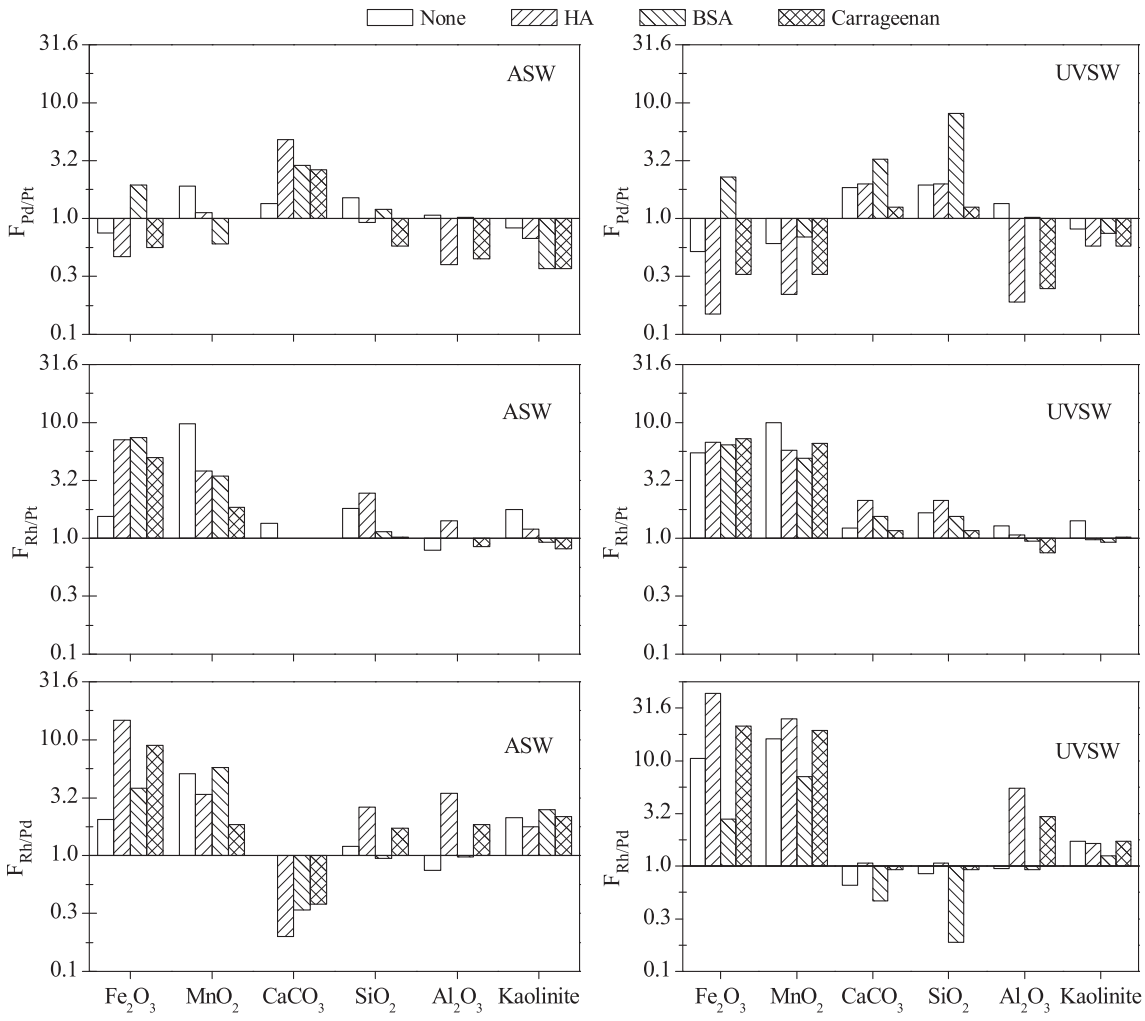

Fig. 4. Fractionation factors between Rh, Pd and Pt during their adsorption onto inorganic particles in the presence or absence of macromolecular organic compounds in different seawater solutions. ASW: artificial seawater; UVSW: UV-irradiated natural seawater; None: the particle systems without macromolecular organic compound; HA: the particle systems with humic acid; BSA: the particle systems with bovine serum albumin; Carrageenan: the particle systems with carrageenan.

HA > BSA ≈ carrageenan and HA ≈ BSA ≈ carrageenan, respectively. Comparatively, the fractionation between Rh and Pt in the process of their adsorption onto the studied particles except for Fe/Mn oxides was changed slightly by MOCs. In some cases, an obvious difference in F values between ASW and UVSW was observed. This may be caused by the residual dissolved organic matter in UVSW, which was the most important distinction between UVSW and ASW. Overall, MOCs played an important role in regulating the adsorption of PGEs onto inorganic particles.

4. Discussion

4.1. Adsorption characteristics of Pt, Pd and Rh onto the microparticles

Based on the results of adsorption coefficient and fractionation factor, it can be found that the adsorption behaviors of PGEs onto particles varied significantly. The mineral particles showed the maximum adsorption propensity (with the log K_d being 4.54–5.75) and fractionation for PGEs, more than other particles used in this study (Figs. 3 and 4). Fe_2O_3 and MnO_2 exhibited similar behavior of preferring to adsorb Rh and it was followed by Pt and Pd. It indicated that the metal oxides/hydroxides particles had a higher affinity to PGEs ions in seawater. This result is consistent with the contents of PGEs in ferromanganese crusts/nodules in the ocean, which had a high level of PGEs (Sun et al., 2006; Guan et al., 2017). The oceanic ferromanganese crusts/nodules show strong enrichment in Pt and Rh and depletion in Pd (Guan et al., 2017), which was consistent with the strong fractionation of Rh-Pd and Rh-Pt that was generated in the process of their adsorption onto Fe/Mn oxides in this research. However, the fractionation between Pt-Pd was not as obvious as that in the natural oceanic ferromanganese crusts/nodules (Guan et al., 2017), which may be caused by the difference in residual dissolved organic matter between UVSW and ASW. To identify this speculation, the zeta potential of each kind of particle in UVSW and ASW was investigated, and the results are shown in Table 2. The absolute value of Fe/Mn oxides in UVSW was lower than in ASW, which means that these particles in UVSW had a stronger affinity with the negatively charged PGEs complexes. Hence, Fe/Mn oxides play a more important role in the scavenging of Pt, Pd and Rh in the ocean than other inorganic particles.

The affinity of biogenic particles with PGEs was weaker than that of the mineral particles (Figs. 3 and 4). And the adsorption behaviors of Pt, Pd and Rh onto SiO_2 and $CaCO_3$ particles were similar, with the log K_d being around 4.11–4.47 (Table S1). However, some subtle differences could still be noticed. In ASW, the

difference in log K_d between PGEs was so small that it could be neglected; while in UVSW, the corresponding log K_d values were higher than in ASW and slightly decreased in the following order: Pd > Rh > Pt, indicating that the residual dissolved organic matter in UVSW may have some effects on the promotion of the adsorption. There was no obvious fractionation between PGEs in the process of their adsorption onto biogenic particles (Fig. 4). As shown in Table 2, the absolute value of zeta potential in SiO_2 and $CaCO_3$ particle systems (around 10 mV) was higher than that in Fe_2O_3 and MnO_2 particle systems (around 2–3 mV), indicating that the interaction between PGEs and biogenic particles could be more stable. Moreover, the difference in zeta potential between SiO_2 and $CaCO_3$ particle systems was not obvious (Table 2), which may demonstrate the inconspicuous differences in the adsorption and fractionation behaviors of PGEs observed between the two biogenic particles. Other studies also found that SiO_2 exhibited similar adsorption behaviors to Rh and Pt ions without being affected by organic matter (Wood, 1996; Takahashi et al., 1999). If this is the case, in the ocean, the fractionation between Pt, Pd and Rh in the process of their adsorption onto biogenic particles would depend largely on the abundance of diatom frustules and the predominant phytoplankton species (Yang et al., 2013). But in reality, the surface of biogenic particles in the ocean is attached by some organic matter such as humic substances, proteins and carbohydrates. These attachments may change the surface properties of the particles, affecting the adsorption of Pt, Pd and Rh onto these particles. In this study, the difference in the results of the single kind of particle experiments and particle-MOC experiments provided a clue to this speculation (Figs. 3 and 4).

Due to their large surface area and ubiquity in marine environments, lithogenic particles may be an important carrier for PGEs. Like that of biogenic particles, Al_2O_3 and kaolinite did not cause obvious fractionation of PGEs in the adsorption process (Fig. 4). From Table 2, it could be found that kaolinite used in this study has the largest specific surface area. For the two kinds of lithogenic particles used in this study, K_d of Rh, Pd and Pt adsorption onto kaolinite was obviously higher than that onto Al_2O_3 (Fig. 3). However, there was no obvious difference in zeta potential between kaolinite and Al_2O_3 in both UVSW and ASW (Table 2). Therefore, specific surface area might be an important factor in the adsorption of PGEs onto lithogenic particles in seawater.

4.2. The roles of macromolecular organic matter

4.2.1. Humic acid

HA, a mixture which has many types of functional groups, is usually regarded as an important component of colloidal organic matter (Xu and Guo, 2017). It can greatly affect the geochemical behavior of trace metals in seawater by providing electron donating groups to their ions (Wood, 1996). In this study, an obvious decrease in the adsorption of PGEs onto Fe/Mn oxides was observed in the presence of HA (Fig. 3 and Table S1). Pd had the greatest decrease, followed by Pt and Rh. This may be related to the adsorption of HA onto the surface of particles and the speciation dynamics of HA and PGEs in seawater (Parfitt et al., 1977; Wood, 1996; Lyubomirova and Djingova, 2011).

As shown in Fig. 5, compared to a single kind of particle system, something obviously attached to the surface of Fe_2O_3 particles in the Fe_2O_3-HA binary system, which should be HA considering there was no other matter. From the image it could be found that HA was bulky and occupied a large portion of the surface area of the particles. Hence, humic acid, mainly with aromatic ring structures (Wood, 1996; Thimsen and Keil, 1998; Vermeer and Koopal, 1998; Kleber et al., 2007), blocked the available surface of Fe/Mn oxide particles (Takahashi et al., 1999; Tombácz et al., 2004; Qin et al., 2015), and weakened the adsorption of Rh, Pd and Pt onto the particles. In addition, irrespective of particles, there were complex interactions between PGEs and HA in seawater (Liu et al., 2019), which implies that HA competes with particles for adsorbing the ions of PGEs in seawater.

The zeta potential change of particles may be another factor of

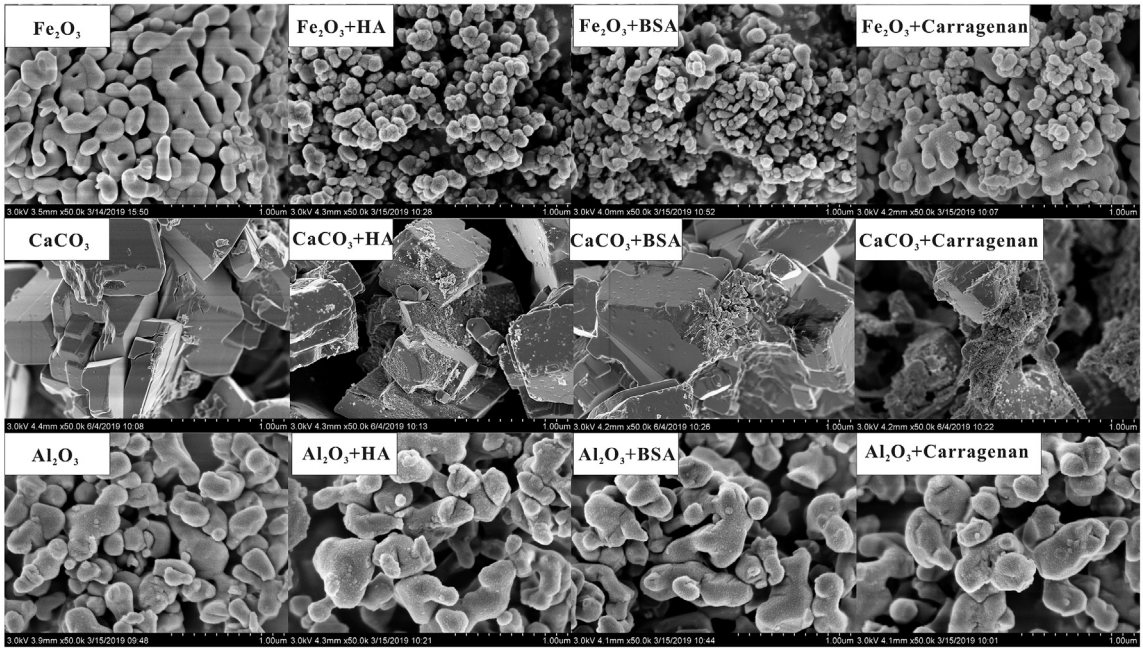

Fig. 5. Scanning electron micrograph of the adsorption of macromolecular organic compounds onto inorganic particles in UV-irradiated natural seawater. Fe_2O_3, $CaCO_3$ and Al_2O_3 in the images represent the single kind of particle systems without organic compound; Fe_2O_3, $CaCO_3$ and Al_2O_3 + HA indicate the particle systems with humic acid; Fe_2O_3, $CaCO_3$ and Al_2O_3 + BSA indicate the particle systems with bovine serum albumin; Fe_2O_3, $CaCO_3$ and Al_2O_3 + carrageenan indicate the particle systems with carrageenan.

influencing the adsorption. The solutions containing Fe_2O_3, $CaCO_3$ and Al_2O_3 were selected for the investigation of the relationship between potential change and adsorption in this study. These particles have some special adsorption characteristics such as the adsorption of PGEs onto Fe_2O_3 exceeds MnO_2, the adsorption of PGEs onto $CaCO_3$ varies significantly, and the adsorption occurring onto Al_2O_3 changes slightly. Therefore, to test the potential change of those particles will be helpful for the understanding of the mechanism of the interactions between particles, organic matter and PGEs. As shown in Fig. 6, the zeta potential for Fe_2O_3 changed from 2.16 mV in the single kind of particle system to −10.8 mV in the particle-MOC binary systems in UVSW. Moreover, it was reported that the potential of inorganic PGEs complexes in natural seawater was negative (Colombo et al., 2008), resulting in the decline of their adsorption onto particles in Fe_2O_3-MOC binary systems (Wood, 1996; Takahashi et al., 1999).

On the whole, when HA was added, a slight decrease in the adsorption of PGEs onto $CaCO_3$ occurred but a slight increase in their adsorption onto SiO_2 occurred in ASW; while the corresponding variations were relatively weaker in UVSW, especially for Rh and Pt. This may be related to the difference in the affinity between HA and particles and the dominated adsorption factors between PGEs and particles. As shown in Fig. 5, an obvious HA attachment on $CaCO_3$ particles could be found. However, although a certain portion of the surface area of $CaCO_3$ particles was occupied by HA, their surface was still dominated by the unoccupied portions. Hence, the adsorption of PGEs onto $CaCO_3$ in this study could be mainly determined by the hydrophobicity and surface area as that reported in the research of Takahashi et al. (1999), even if the zeta potential of this particle changed from 10.8 mV to −8.27 mV in the presence of HA (Fig. 6). In addition, the relatively low adsorption affinity of PGEs onto biogenic particles may be another factor (Fig. 4 and Table S2), which means that the amount of PGEs in this study could be sufficient to support the adsorption by both HA and biogenic particles.

The adsorption characteristics of PGEs onto the lithogenic particles showed a similar contradictory trend with that of the biogenic particles but varied between elements. For Rh and Pt, HA promoted their distribution onto Al_2O_3 particles, however, it showed an inhibitory effect for Pd, which may be caused by the interaction between HA and the particles being reported in literature (e.g. Fein et al., 1999; Tombácz et al., 2004; Feng et al., 2005; Wang and Xing, 2005; Janot et al., 2012). Shown by the SEM image in Fig. 5, there was no obvious HA attachment observed on the surface of Al_2O_3 particles. However, HA could produce thick coronas as adsorbed layers, which were covered with a large number of different polar groups, around Al_2O_3 particles in seawater (Ghosh et al., 2010). PGEs in solutions might react firstly with the polar groups on the thick corona around the surface of Al_2O_3 particle. Therefore, the inhibitory effect may be related to the positive or negative electrical characteristics of HA corona. The zeta potential of the solutions with Al_2O_3 particles was negative, and it changed from −4.64 to −12.3 mV when HA was added (Fig. 6), indicating the increase of repellant between the particle surface and PGEs. For kaolinite, the inhibition effect of HA on the adsorption of PGEs could be deduced. The interaction between the HA modified kaolinite particle surface and PGEs ions was speculated to be more like a chelating ion-exchange rather than a simple inorganic ion exchange, which was similar to that reported in Jülide and Apak (2006). Therefore, the adsorption of PGEs onto kaolinite particles decreased in the presence of HA, may be due to its broad combination with the −COO or −C═O groups in humic acid (Wood, 1996). However, the interactions among PGEs, tested particles and HA involve complicated specific molecular mechanisms which are beyond the scope of this research, and further research is needed for the understanding of the processes.

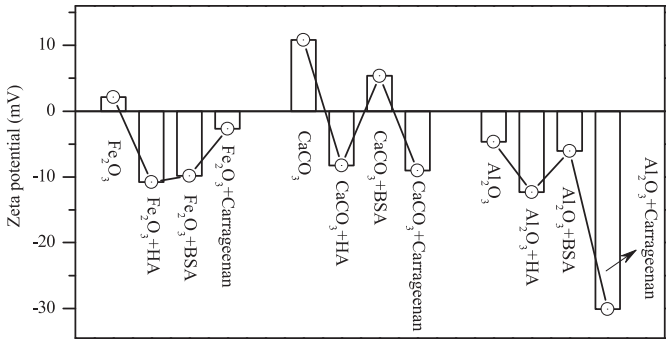

Fig. 6. Zeta potential of UV-irradiated natural seawater in the presence of different inorganic particles and organic compounds.

4.2.2. Bovine serum albumin

Like HA, BSA also changed the adsorption characteristics of Pt, Pd and Rh onto different particles (Figs. 3 and 4). For some particles, their morphology could be significantly altered by BSA adhering onto their surface (Liang and Wang, 2010; Rezwan et al., 2004; Song et al., 2012). These BSA-coated particles weakened the direct interaction between PGEs and the particles in solutions (Wisniewska et al., 2015; Givens et al., 2017). In this research, BSA showed an inhibition effect on the adsorption of Rh and Pt onto mineral particle Fe_2O_3 and MnO_2, which was similar to that of HA (Fig. 3 and Table S1). The SEM images show a similar adsorption feature of HA and BSA interacting with Fe_2O_3 particles (Fig. 5), and the log K_d and zeta potential values of the Fe_2O_3-BSA system were comparable to those of the Fe_2O_3-HA system (Figs. 3 and 6), which provided a clue that the adsorption behavior of Rh and Pt onto Fe_2O_3 particles in the presence of HA and BSA may be similar.

For the tested biogenic and lithogenic particles, in the presence of BSA, the log K_d values of PGEs onto all of them were approximately around 4 except for Pd onto $CaCO_3$ and kaolinite (Fig. 3). Shown by the SEM images, the adsorption feature of BSA onto $CaCO_3$ and Al_2O_3 particles was similar (Fig. 5). Moreover, compared to their corresponding values of the single kind of particle systems, the zeta potential of BSA-$CaCO_3$ and -Al_2O_3 binary systems changed smaller than that of HA-$CaCO_3$ and -Al_2O_3 binary systems (Fig. 6). It indicated that the adsorption of Rh and Pt onto these two kinds of particles may be dominated by the hydrophobicity/hydrophilicity and/or available surface area of the particles even in the presence of BSA. The adsorption behavior of Pd onto Fe/Mn oxides, $CaCO_3$ and kaolinite particles was different from Pt and Rh in the presence of BSA, which was possibly controlled by the distinction in their ability of interacting with BSA reflected by their partition and fractionation features (Figs. 3 and 4). In BSA-particle binary system, the inhibition effect of BSA on the adsorption of Pd onto the particles was smaller than that of HA, which was consistent with the results of the previous research that the interaction between BSA and Pd was weaker than that between HA and Pd (Liu et al., 2019).

4.2.3. Carrageenan

Like that of HA and BSA, carrageenan inhibited the adsorption of Rh and Pt onto mineral particles Fe_2O_3 and MnO_2 (Fig. 2 and Table S2). Compared to the corresponding system free of MOCs, the change of zeta potential of the Fe_2O_3 particle system in the presence of carrageenan was smaller than that of HA and BSA (Fig. 6). And carrageenan did not adhere to the Fe_2O_3 particles as significantly as that of HA and BSA, reflected by the SEM image (Fig. 5). These provided a clue that the direct interaction between

carrageenan micelles and PGEs would compete with and weaken the adsorption of PGEs onto Fe_2O_3.

The biogenic particles had a higher adsorption constant of PGEs than the lithogenic particles, and the log K_d values of PGEs in either of $CaCO_3$ and SiO_2 systems with and without carrageenan were close (Fig. 3), which indicated that carrageenan did not obviously affect the adsorption of PGEs onto biogenic particles. This may be the case because polysaccharides may not adsorb easily onto the particles with acidic surfaces such as SiO_2 (Liu et al., 2000; Laskowski et al., 2007). Besides, the SEM images show that only a very small amount of carrageenan attached to the surface of $CaCO_3$ and Al_2O_3. Therefore, for the biogenic and lithogenic particles used in the experiment, if there were no direct interactions between PGEs and carrageenan, the addition of carrageenan may have little influence on the adsorption of PGEs onto them, and the adsorption behavior of PGEs onto these particles with and without carrageenan should be similar. However, PGEs showed various adsorption behaviors onto biogenic and lithogenic particles according to the experimental results (Figs. 3 and 4). The degree of difference in log K_d values of Pt, Pd and Rh between the single kind of biogenic and lithogenic particle system and its corresponding carrageenan-particle binary system followed the order of Pt < Rh < Pd.

The results of zeta potential measurement showed that the values of the $CaCO_3$ and Al_2O_3 single kind of particle systems changed greatly from 10.8 to −9.01 mV and −4.64 to −30.1 mV respectively when carrageenan was added, indicating an increase in affinity to cations caused by carrageenan. A strong interaction between Pd and Rh ions and carrageenan was found in Liu et al. (2019). Therefore, the formation of PGEs-carrageenan complexes in carrageenan-biogenic and -lithogenic particle binary systems may influence the adsorption of PGEs onto particles greatly.

4.3. Mechanism of MOCs affecting PGEs adsorption onto inorganic particles in seawater

As discussed in Sections 4.1 and 4.2, MOCs significantly influenced the adsorption of Pt, Pd and Rh onto inorganic particles in seawater by the interactions among MOCs, particles and PGEs. As shown in Fig. 7, a possible mechanism of MOCs affecting the adsorption of PGEs onto inorganic particles in seawater could be obtained. In the following, three key processes of interactions which occurred in the particle-MOC binary systems were proposed based on the experimental results of this research and previous reports. First, PGEs interacted directly with particles like those of the single kind of particle system, in which the interaction was mainly determined by the physicochemical properties of PGEs and particles. Second, the interaction occurred between PGEs and MOCs in seawater (Wood, 1996; Sures and Zimmermann, 2007). PGEs could form stable complexes with MOCs and inorganic and small molecule organic ligands (Wood, 1996; Cobelo-García, 2013), which inhibited the adsorption of PGEs onto particles. Third, the competitive adsorption occurred between PGEs-MOCs and PGEs-particles. MOCs and the colloids they formed could adsorb PGEs in seawater (Zakharova, 1987; Liu et al., 2019), which led to a reduction in the distribution of PGEs onto the inorganic particles through the competitive adsorption. In addition, the presence of MOCs in the solution could change the surface properties of the particles (Fein et al., 1999; Tombácz et al., 2004; Feng et al., 2005; Janot et al., 2012; Sanderman et al., 2014). By adsorbing different kinds of MOCs, the surface potential and the area of the particles were changed (Figs. 5–7), which could directly affect the adsorption of PGEs. Besides, the attachment increased the macromolecular structure on the particle surface (Fig. 5), causing a reduction in macromolecules in the dissolved phase (Tombácz et al., 2004; Feng et al., 2005; Janot et al., 2012). On the whole, MOCs inhibited the adsorption of Pt, Pd and Rh onto inorganic particles in seawater in most instances and changed the fractionation of them.

5. Conclusions

In this research, controlled laboratory experiments were conducted to examine the adsorption characteristics of Pt, Pd and Rh ions onto inorganic particles. The results show that the chemical composition of particles played an important role in scavenging of Pt, Pd and Rh in seawater in a single kind of particle system. The representative mineral particles Fe_2O_3 and MnO_2 had the highest

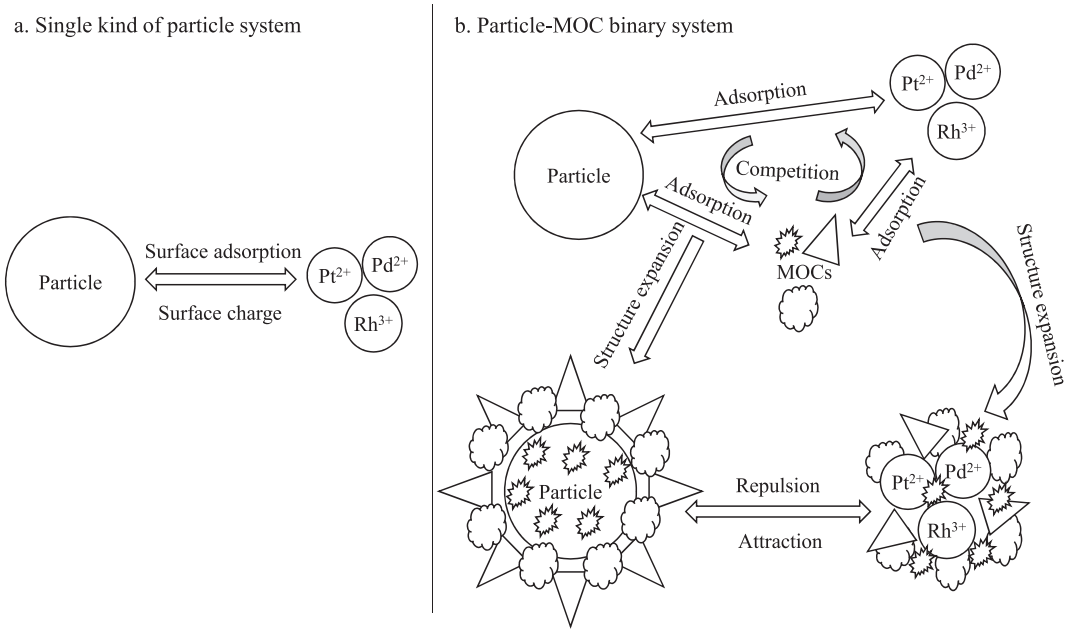

Fig. 7. Possible process of the adsorption of Pt, Pd and Rh onto inorganic microparticles in seawater with single kind of particle (a) and particle-MOC binary components (b).

degree of affinity with PGEs, followed by biogenic particles SiO_2 and $CaCO_3$ and lithogenic particle kaolinite, and lithogenic particle Al_2O_3 had the lowest adsorption capacity. The adsorption behavior of Pt, Pd and Rh in artificial seawater and UV irradiated natural seawater was different to an extent, which was possibly caused by the residual organic matter in the latter.

Macromolecular organic compounds (MOCs), including HA, BSA and carrageenan, changed the adsorption characteristics of Pt, Pd and Rh onto inorganic particles greatly. For Pt, MOCs inhibited its adsorption onto inorganic particles. For Pd, the effects of MOCs varied significantly with the particles, indicating complex interactions among Pd, MOCs and particles. For Rh, the effects of MOCs were similar to that of Pt in the presence of MOCs, except for Fe_2O_3 and MnO_2 which indicated a more important role in scavenging of Rh. The presence of MOCs did not obviously change the adsorption feature of Pd onto biogenic particles; however, MOCs inhibited its adsorption onto mineral and lithogenic particles and the influence varied significantly. In summary, the results of this research suggest that the presence and type of macromolecular organic compounds are crucial in regulating the interactions between Pt, Pd and Rh ions and inorganic microparticles.

Conflicts of interest

We declare that we have no conflicts of interest to this work.

Acknowledgement

We would like to thank Yuxi Lu and Tianci Gao for their field and laboratory assistance, helpful advice and in-depth discussion. This study was funded by the National Natural Science Foundation of China (41376083).

Appendix A. Supplementary data

Supplementary data to this article can be found online at https://doi.org/10.1016/j.envpol.2019.113192.

References

Baker, A., Spencer, R.G.M., 2004. Characterization of dissolved organic matter from source to sea using fluorescence and absorbance spectroscopy. Sci. Total Environ. 333 (1–3), 217–232.
Clement, N., Muresan, B., Hedde, M., Francois, D., 2015. Assessment of palladium footprint from road traffic in two highway environments. Environ. Sci. Pollut. Res. 22 (24), 20019–20031.
Cobelo-García, A., 2013. Kinetic effects on the interactions of Rh(III) with humic acids as determined using size-exclusion chromatography (SEC). Environ. Sci. Pollut. Res. 20 (4), 2330–2339.
Cobelo-García, A., Lopez-Sanchez, D.E., Almecija, C., Santos-Echeandia, J., 2013. Behavior of platinum during estuarine mixing (Pontevedra Ria, NW Iberian Peninsula). Mar. Chem. 150 (2), 11–18.
Cobelo-García, A., Lopez-Sanchez, D.E., Schafer, J., Petit, J.C.J., Blanc, G., Turner, A., 2014. Behavior and fluxes of Pt in the macrotidal Gironde estuary (SW France). Mar. Chem. 167, 93–101.
Cobelo-García, A., Turner, A., Millward, G.E., 2008. Fractionation and reactivity of platinum group elements during estuarine mixing. Environ. Sci. Technol. 42 (4), 1096-1011.
Colombo, C., Oates, C.J., Monhemius, A.J., Plant, J.A., 2008. Complexation of platinum, palladium and rhodium with inorganic ligands in the environment. Geochem. Explor. Environ. Anal. 8 (1), 91–101.
Djingova, R., Heidenreich, H., Kovacheva, P., Markert, B., 2003. On the determination of platinum group elements in environmental materials by inductively coupled plasma mass spectrometry and microwave digestion. Anal. Chim. Acta 489 (2), 245–251.
Ek, K.H., Morrison, G.M., Rauch, S., 2004. Environmental routes for platinum group elements to biological materials - a review. Sci. Total Environ. 334–335, 21–38.
Fein, J.B., Boily, J.F., Güçlü, K., Kaulbach, E., 1999. Experimental study of humic acid adsorption onto bacteria and Al-oxide mineral surfaces. Chem. Geol. 162 (1), 33–45.
Feng, X.J., Simpson, A.J., Simpson, M.J., 2005. Chemical and mineralogical controls on humic acid sorption to clay mineral surfaces. Org. Geochem. 36 (11), 1553–1566.
Fornieles, A.C., de Torres, A., Alonso, E.V., Pavon, J.M.C., 2016. Simultaneous determination of traces of Pt, Pd, and Ir by SPE-ICP-OES. Test for chemical vapor generation. Microchem. J. 124, 82–89.
Ghosh, S., Mashayekhi, H., Bhowmik, P., Xing, B.S., 2010. Colloidal stability of Al_2O_3 nanoparticles as affected by coating of structurally different humic acids. Langmuir 26 (2), 873–879.
Givens, B.E., Xu, Z., Fiegel, J., Grassian, V.H., 2017. Bovine serum albumin adsorption on SiO_2 and TiO_2 nanoparticle surfaces at circumneutral and acidic pH: a tale of two nano-bio surface interactions. J. Colloid Interface Sci. 493, 334–341.
Guan, Y., Sun, X.M., Ren, Y.Z., Jiang, X.D., 2017. Mineralogy, geochemistry and genesis of the polymetallic crusts and nodules from the South China Sea. Ore Geol. Rev. 89, 106–117.
Gueguen, C., Guo, L.D., Wang, D., Tanaka, N., Hung, C.C., 2006. Chemical characteristics and origin of dissolved organic matter in the Yukon River. Biogeochemistry 77 (2), 139–155.
Honeyman, B.D., Santschi, P.H., 1989. A Brownian-pumping model for oceanic trace metal scavenging: evidence from Th isotopes. J. Mar. Res. 47 (4), 951–992.
Ilina, S.M., Drozdova, O.Y., Lapitskiy, S.A., Alekhin, Y.V., Demin, V.V., Zavgorodnyaya, Y.A., Shirokova, L.S., Viers, J., Pokrovsky, O.S., 2014. Size fractionation and optical properties of dissolved organic matter in the continuum soil solution-bog-river and terminal lake of a boreal watershed. Org. Geochem. 66 (1), 14–24.
Janot, N., Reiller, P.E., Zheng, X., Croué, J.P., Benedetti, M.F., 2012. Characterization of humic acid reactivity modifications due to adsorption onto α-Al_2O_3. Water Res. 46 (3), 731–740.
Jülide, H., Apak, R., 2006. Modeling of copper(II) and lead(II) adsorption on kaolinite-based clay minerals individually and in the presence of humic acid. J. Colloid Interface Sci. 295 (1), 1–13.
Kleber, M., Sollins, P., Sutton, R., 2007. A conceptual model of organo-mineral interactions in soils: self-assembly of organic molecular fragments into zonal structures on mineral surfaces. Biogeochemistry 85 (1), 9–24.
Koek, M., Kreuzer, O.P., Maier, W.D., Porwal, A.K., Thompson, M., Guj, P., 2010. A review of the PGM industry, deposit models and exploration practices: implications for Australia's PGM potential. Resour. Policy 35 (1), 20–35.
Lardinois, D., Eism, D., Chen, S., 1995. Seasonal differences in concentrations of particulate lipids, proteins and chitin in the north-sea. Neth. J. Sea Res. 33 (2), 147–161.
Laskowski, J.S., Liu, Q., O'Connor, C.T., 2007. Current understanding of the mechanism of polysaccharide adsorption at the mineral/aqueous solution interface. Int. J. Miner. Process. 84 (1–4), 59–68.
Li, L., Liu, J., Wang, X., Shi, X., 2015. Dissolved trace metal distributions and Cu speciation in the southern Bohai Sea, China. Mar. Chem. 172, 34–45.
Liang, H.F., Wang, Z.C., 2010. Adsorption of bovine serum albumin on functionalized silica-coated magnetic $MnFe_2O_4$ nanoparticles. Mater. Chem. Phys. 124 (2–3), 964–969.
Lin, P., Chen, M., Guo, L.D., 2015. Effect of natural organic matter on the adsorption and fractionation of thorium and protactinium on nanoparticles in seawater. Mar. Chem. 173, 291–301.
Lin, P., Guo, L.D., Chen, M., 2014. Adsorption and fractionation of thorium and protactinium on nanoparticles in seawater. Mar. Chem. 162, 50–59.
Liu, J., Yu, Z.G., Zang, J.Y., Sun, T., Zhao, C.Y., Ran, X.B., 2015. Distribution and budget of organic carbon in the Bohai and Yellow Seas. Adv. Earth Sci. 30 (5), 564–578.
Liu, K., Gao, X.L., Xing, Q.G., Chen, F.S., 2019. Adsorption kinetics of platinum group elements onto macromolecular organic matter in seawater. Acta Oceanol. Sin. 38 (8), 8–16.
Liu, Q., Zhang, Y., Laskowski, J.S., 2000. The adsorption of polysaccharides onto mineral surfaces: an acid/base interaction. Int. J. Miner. Process. 60 (3–4), 229–245.
Lyubomirova, V., Djingova, R., 2011. Identification of Pt and Pd bound to humic acid species in spiked soils and street dusts by size exclusion chromatography and ICP-MS. Chem. Speciat. Bioavailab. 23 (1), 38–45.
Mashio, A.S., Obata, H., Tazoe, H., Tsutsumi, M., Santos, A.F.I., Gamo, T., 2016. Dissolved platinum in rainwater, river water and seawater around Tokyo Bay and Otsuchi Bay in Japan. Estuar. Coast Shelf Sci. 180, 160–167.
Merget, R., Rosner, G., 2001. Evaluation of the health risk of platinum group metals emitted from automotive catalytic converters. Sci. Total Environ. 270 (1–3), 165–173.
Mitra, A., Sen, I.S., 2017. Anthrobiogeochemical platinum, palladium and rhodium cycles of earth: emerging environmental contamination. Geochem. Cosmochim. Acta 216, 417–432.
Mudd, G.M., 2012. Key trends in the resource sustainability of platinum group elements. Ore Geol. Rev. 46 (2), 106–117.
Parfitt, R.L., Fraser, A.R., Farmer, V.C., 1977. Adsorption on hydrous oxides. III. Fulvic acid and humic acid on goethite, gibbsite and imogolite. J. Soil Sci. 28 (2), 289–296.
Pawlak, J., Lodyga-Chrucinska, E., Chrustowicz, J., 2014. Fate of platinum metals in the environment. J. Trace Elem. Med. Biol. 28 (3), 247–254.
Qin, X., Liu, F., Wang, G., Huang, G., 2015. Adsorption of humic acid from aqueous solution by hematite: effects of pH and ionic strength. Environ. Earth Sci. 73, 4011–4017.
Ran, L., Lu, X.X., Sun, H., Han, J., Li, R., Zhang, J., 2013. Spatial and seasonal variability of organic carbon transport in the Yellow River, China. J. Hydrol 498, 76–88.
Rao, C.R.M., Reddi, G.S., 2000. Platinum group metals (PGM); occurrence, use and recent trends in their determination. Trac. Trends Anal. Chem. 19 (9), 565–586.

Reith, F., Campbell, S.G., Ball, A.S., Pring, A., Southam, G., 2014. Platinum in Earth surface environments. Earth Sci. Rev. 131 (4), 1–21.
Rezwan, K., Meier, L.P., Rezwan, M., Voros, J., Textor, M., Gauckler, L.J., 2004. Bovine serum albumin adsorption onto colloidal Al_2O_3 particles: A new model based on zeta potential and UV–Vis measurements. Langmuir 20 (23), 10055–10061.
Roberts, K.A., Xu, C., Hung, C.C., Conte, M.H., Santschi, P.H., 2009. Scavenging and fractionation of thorium vs. protactinium in the ocean, as determined from particle–water partitioning experiments with sediment trap material from the Gulf of Mexico and Sargasso Sea. Earth Planet. Sci. Lett. 286 (1–2), 131–138.
Ruchter, N., Sures, B., 2015. Distribution of platinum and other traffic related metals in sediments and clams (*Corbicula* sp.). Water Res. 70, 313–324.
Sanderman, J., Maddern, T., Baldock, J., 2014. Similar composition but differential stability of mineral retained organic matter across four classes of clay minerals. Biogeochemistry 121 (2), 409–424.
Šebek, O., Mihaljevic, M., Strnad, L., Ettler, V., Jezek, J., Stedry, R., Drahota, P., Ackerman, L., Adamec, V., 2011. Dissolution kinetics of Pd and Pt from automobile catalysts by naturally occurring complexing agents. J. Hazard Mater. 198 (2), 331–339.
Song, L., Yang, K., Jiang, W., Du, P., Xing, B., 2012. Adsorption of bovine serum albumin on nano and bulk oxide particles in deionized water. Colloid. Surface. B 94 (6), 341–346.
Sorensen, S.N., Engelbrekt, C., Lutzhoft, H.C.H., Jimenez-Lamana, J., Noori, J.S., Alatraktchi, F.A., Delgado, C.G., Slaveykova, V.I., Baun, A., 2016. A multimethod approach for investigating algal toxicity of platinum nanoparticles. Environ. Sci. Technol. 50 (19), 10635–10643.
Speder, J., Zana, A., Spanos, I., Kirkensgaard, J.J.K., Mortensen, K., Hanzlik, M., Arenz, M., 2014. Comparative degradation study of carbon supported proton exchange membrane fuel cell electrocatalysts – the influence of the platinum to carbon ratio on the degradation rate. J. Power Sources 261, 14–22.
Sucha, V., Mihaljevic, M., Ettler, V., Strnad, L., 2016. The pH-dependent release of platinum group elements (PGEs) from gasoline and diesel fuel catalysts: implication for weathering in soils. J. Environ. Manag. 171, 52–59.
Sun, X.M., Xue, T., He, G.W., Zhang, M., Shi, G.Y., Wang, S.W., Lu, H.F., 2006. Platinum group elements (PGE) and Os isotopic geochemistry of ferromanganese crusts from Pacific Ocean seamounts and their constraints on genesis. Acta Petrol. Sin. 22 (12), 3014–3026.
Sures, B., Zimmermann, S., 2007. Impact of humic substances on the aqueous solubility, uptake and bioaccumulation of platinum, palladium and rhodium in exposure studies with *Dreissena polymorpha*. Environ. Pollut. 146 (2), 444–451.
Suzuki, A., Obata, H., Okubo, A., Gamo, T., 2014. Precise determination of dissolved platinum in seawater of the Japan sea, sea of okhotsk and western north Pacific ocean. Mar. Chem. 166, 114–121.
Takahashi, Y., Minai, Y., Ambe, S., Makide, Y., Ambe, F., 1999. Comparison of adsorption behavior of multiple inorganic ions on kaolinite and silica in the presence of humic acid using the multitracer technique. Geochem. Cosmochim. Acta 63 (6), 815–836.
Thimsen, C.A., Keil, R.G., 1998. Potential interactions between sedimentary dissolved organic matter and mineral surfaces. Mar. Chem. 62 (1–2), 65–76.
Tombácz, E., Libor, Z., Illés, E., Majzik, A., Klumpp, E., 2004. The role of reactive surface sites and complexation by humic acids in the interaction of clay mineral and iron oxide particles. Org. Geochem. 35 (3), 257–267.
Turner, A., Crussell, M., Millward, G.E., Cobelo-Garcia, A., Fisher, A.S., 2006. Adsorption kinetics of platinum group elements in river water. Environ. Sci. Technol. 40 (5), 1524–1531.
Turner, A., Wu, K.T., 2007. Removal of platinum group elements in an estuarine turbidity maximum. Mar. Chem. 107 (3), 295–307.
Vermeer, A.W.P., Koopal, L.K., 1998. Adsorption of humic acid to mineral particles. I. Specific and electrostatic interactions. Langmuir 14 (10), 2810–2819.
Wang, K., Xing, B.S., 2005. Structural and sorption characteristics of adsorbed humic acid on clay minerals. J. Environ. Qual. 34 (1), 342–349.
Wiseman, C.L.S., Zereini, F., 2009. Airborne particulate matter, platinum group elements and human health: a review of recent evidence. Sci. Total Environ. 407 (8), 2493–2500.
Wisniewska, M., Szewczuk-Karpisz, K., Sternik, D., 2015. Adsorption and thermal properties of the bovine serum albumin–silicon dioxide system. J. Therm. Anal. Calorim. 120 (2), 1355–1364.
Wood, S.A., 1996. The role of humic substances in the transport and fixation of metals of economic interest (Au, Pt, Pd, U, V). Ore Geol. Rev. 11 (95), 1–31.
Xu, H.C., Guo, L.D., 2017. Molecular size-dependent abundance and composition of dissolved organic matter in river, lake and sea waters. Water Res. 117, 115–126.
Yang, W.F., Guo, L.D., Chuang, C.Y., Santschi, P.H., Schumann, D., Ayranov, M., 2015. Influence of organic matter on the adsorption of Pb-210, Po-210, Be-7 and their fractionation on nanoparticles in seawater. Earth Planet. Sci. Lett. 423, 193–201.
Yang, W.F., Guo, L.D., Chuang, C.Y., Schumann, D., Ayranov, M., Santschi, P.H., 2013. Adsorption characteristics of ^{210}Pb, ^{210}Po and ^{7}Be onto micro-particle surfaces and the effects of macromolecular organic compounds. Geochem. Cosmochim. Acta 107, 47–64.
Zakharova, I.A., 1987. Coordination compounds of Pd(II) and Pt(II) with thiodiacetic acid. Polyhedron 6 (5), 1065–1070.
Zimmermann, S., Wolff, C., Sures, B., 2017. Toxicity of platinum, palladium and rhodium to *Daphnia magna* in single and binary metal exposure experiments. Environ. Pollut. 224, 368–376.